A Two-Level Strategy to Realize Life-Cycle Production Optimization in an Operational Setting

G.M. van Essen, SPE, Delft University of Technology; **P.M.J. Van den Hof,** Delft University of Technology, Eindhoven University of Technology; and **J.-D. Jansen,** SPE, Delft University of Technology

Summary

We present a two-level strategy to improve robustness against uncertainty and model errors in life-cycle flooding optimization. At the upper level, a physics-based large-scale reservoir model is used to determine optimal life-cycle injection and production profiles. At the lower level, these profiles are considered as set points (reference values) for a tracking control algorithm, also known as a model predictive controller (MPC), to optimize the production variables over a short moving horizon on the basis of a simple data-driven model. In the process industry such a two-level approach is a well-known strategy to correct for small local disturbances that may have a negative (cumulative) effect on the long-term production strategy. We used a conventional reservoir simulator with gradient-based optimization functionality to perform the life-cycle optimization. Next, we applied this long-term strategy to a reservoir model, representing the truth, with somewhat different geological characteristics and near-wellbore characteristics not captured in the reservoir model used for the long-term optimization. We compared the performance (oil recovery) of this truth model when applying the life-cycle strategy with and without the corrections provided by the data-driven algorithm and the tracking controller. In this theoretical study we observed that the use of the lower-level controller enabled successful tracking of the reference values provided by the upper-level optimizer. In our example, a performance drop of 6.4% in net present value (NPV), caused by differences between the reservoir model used for life-cycle optimization and the true reservoir, was successfully reduced to only 0.5% when applying the two-level strategy. Several studies have demonstrated that model-based life-cycle production optimization has a large scope to improve long-term economic performance of waterflooding projects. However, because of uncertainties in geology, economics, and operational decisions, such life-cycle strategies cannot simply be applied in reality. Our two-level approach offers a potential solution to realize life-cycle optimization in an operational setting.

Introduction

Several studies have shown that there is considerable scope to improve reservoir management with reservoir models for the optimization of economic life-cycle performance. This type of model-based life-cycle optimization is also referred to as flooding optimization, recovery optimization, sweep optimization, or production optimization, although the latter name is conventionally reserved for more-short-term operational optimization without the use of a reservoir-simulation model. A very efficient way to perform model-based life-cycle optimization is with the aid of gradient-based methods where the gradient is obtained through an adjoint technique (Asheim 1988, Sudaryanto and Yortsos 2000, Brouwer and Jansen 2004, Sarma et al. 2005, or Kraaijevanger et al. 2007). For further references we refer to the review paper by Jansen (2011). Alternative methods, which are generally less efficient but much easier to implement, use a variety of methods such as streamline techniques (Alhuthali et al. 2007); approximate-gradient methods such as ensemble techniques (Chen et al. 2009; Su and Oliver 2010) or stochastic techniques (Wang et al. 2009); or truly gradient-free methods including evolutionary techniques (Almeida et al. 2007) and pattern-based search algorithms (Echeverría Ciaurri et al. 2011). In all these studies the objective function is typically ultimate recovery or NPV, whereas the controllable input is a set of well controls in the form of prescribed bottomhole pressures, flow rates, or valve settings. In practice, the optimal inputs, as obtained from the optimization, cannot be directly applied in production operations because

(1) There is uncertainty in reservoir flow parameters, and the real reservoir response will always be different from the simulated response.

(2) The optimal inputs, in terms of life-cycle economic performance, are often suboptimal during the early phase of reservoir production in terms of instantaneous production rates.

(3) Reservoir-simulation models are usually much too coarse to represent near-wellbore reservoir dynamics such as gas or water coning.

(4) Unforeseen operational activities, such as breakdown maintenance or well interventions, cannot be accounted for in the reservoir simulator.

To a certain extent, the first limitation—the effect of uncertainties in the reservoir flow parameters—can be counteracted by performing the optimization in a "robust" fashion by use of an ensemble of reservoir models (van Essen et al. 2009). A further step to counteract uncertainties is through frequent model updating with the aid of computer-assisted history matching (CAHM). Such a combination of life-cycle optimization and CAHM is sometimes called closed-loop reservoir management (CLRM) or closed-loop production optimization, and we refer the reader to Naevdal et al. (2006), Sarma et al. (2008), Chen et al. (2009), Jansen et al. (2009), and Wang et al. (2009) for further information. The second limitation—the suboptimal nature, from a production perspective, of optimal life-cycle settings—can to a certain extent be alleviated by sequential optimization or multiobjective optimization (van Essen et al. 2011 or Chen et al. 2012). However, the third and fourth limitations are often too local (either in time or in space) to be captured in a reservoir-simulation model, but may nevertheless have a negative (cumulative) effect on the life-cycle performance. Moreover, CAHM, and therefore CLRM, are usually time-consuming exercises that may limit how frequently the reservoir model can be updated.

Multilevel Optimization and Control

Similar difficulties to practical implementation of long-term optimal control strategies occur in the process industry, and the standard solution is to use a multilevel control structure in which the results of a higher level serve as optimal reference for the next lower level. Such a "disturbance rejection" strategy can quickly correct for small local disturbances that may have a negative (cumulative) effect on the long-term production strategy. Similar multilevel control structures have been proposed by Saputelli et al. (2006) and Foss and Jensen (2010) for use in upstream oil

This paper (SPE 149736) was accepted for presentation at the SPE Intelligent Energy International, Jaarbeurs, Utrecht, the Netherlands, 27–29 March 2012, and revised for publication. Original manuscript received for review 17 May 2012. Revised manuscript received for review 19 March 2013. Paper peer approved 19 April 2013.

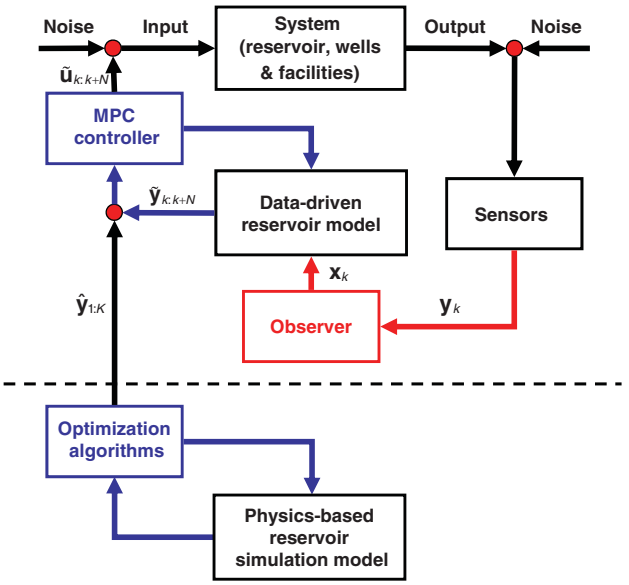

Fig. 1—Two-level strategy to combine life-cycle optimization (bottom part of the figure) with MPC tracking of production (top part of the figure).

and gas operations. The latter paper describes a four-level structure that makes a distinction between asset management, reservoir management, production optimization, and control and automation. Here we consider the second and the third level. At the second level, we apply model-based life-cycle optimization to a single reservoir model. At the third level, we use a relatively simple data-driven model in combination with a tracking control algorithm to determine well settings in the production-optimization domain. We note that in similar control structures in the process industry, the second and third levels are often referred to as dynamic real-time optimization and model predictive control (MPC), respectively.

Fig. 1 represents a schematic of our proposed two-level strategy. The box at the very top of the figure represents the system consisting of reservoir, wells, and facilities. The boxes at the bottom of the figure (below the dotted line) represent the reservoir-simulation model and the life-cycle optimization tool. The other boxes, above the dotted line, represent elements of the model-predictive production control. Their meaning will be described in detail.

Reservoir Modeling By Use of Linear Data-Driven Models

The introduction of advanced (subsurface) production measurement devices in new wells has opened the way for data-driven modeling techniques. The measurement frequency of these devices is quite high (on the order of seconds to minutes) in relation to the timestep size of physics-based reservoir-simulation models (on the order of days to months). Before the data are assimilated into these simulation models, they are therefore resampled and post-processed to match the timestep size, by which all information on fast, localized dynamics is lost. However, by use of the high-resolution data in data-driven modeling, the fast dynamics is captured such that short-term predictions are better in comparison with those of physics-based reservoir models. There exists a wide variety of data-driven modeling methods that create a model on the basis of the input and output data it has been given, such as neural networks, genetic algorithms, or polynomial interrelations. Early attempts to apply data-driven modeling techniques to hydrocarbon reservoirs have been described by Rowan and Clegg (1963) and Chierici et al. (1981), whereas more-recent attempts include extended Kalman filtering (Liu et al. 2009) and capacitance-resistance modeling (Sayarpour et al. 2009).

We use a system-identification technique to determine a linear data-driven model. System identification, which has its origins in the downstream oil industry, is a black-box method, creating a model solely on the basis of measured data (Ljung 1999). The order of the (linear) model (i.e., the number of dominant dynamic degrees of freedom represented in the identified model) is inferred from the data itself. During the modeling process the order of the model is increased until the residual error between modeled and measured data shows no evidence (within a predefined tolerance) of uncaptured dynamics. We note that the parameters of such an identified model usually have no direct physical interpretation and can therefore not be used to update the parameters of the physics-based reservoir model used for the life-cycle optimization. In the example presented in this paper, a special subclass of system identification, subspace identification (SubID), has been used. SubID was used because of its simple structure, which is well suited for multiple-input/multiple-output systems, and its computational efficiency. A conceptual description of the method is given in Appendix A, whereas for further information we refer the reader to Viberg (1995) and Van Overschee and De Moor (1996). Earlier SubID applications to reservoir modeling are discussed by Markovinovic et al. (2002) and Heijn et al. (2004).

The data-driven model determined through SubID was subsequently used as a prediction model for the model predictive controller. In the example described in this paper, we consider a reservoir with eight water-injection wells and four production wells, each equipped with devices to measure total flow rates (i.e., the sum of oil and water rates) and downhole pressures. We chose an input vector with 12 elements:

$$\begin{aligned}\mathbf{u} &= [u_1 \quad u_2 \quad \cdots \quad u_{12}]^T \\ &= [p_{wf,1} \quad p_{wf,2} \quad p_{wf,3} \quad p_{wf,4} \quad | \quad q_{wi,5} \quad q_{wi,6} \quad \cdots \quad q_{wi,12}]^T, \end{aligned} \qquad \cdots\cdots\cdots\cdots\cdots\cdots (1)$$

where $p_{wf,1}, \ldots, p_{wf,4}$ represent the bottomhole pressures in the producers, and $q_{w,5}, \ldots, q_{w,12}$ are the flow rates in the injectors. The output vector was chosen as

$$\mathbf{y} = [y_1 \quad y_2 \quad y_3 \quad y_4]^T = [q_{t,1} \quad q_{t,2} \quad q_{t,3} \quad q_{t,4}]^T, \quad \ldots\ldots (2)$$

where the four elements $q_{t,1}, \ldots, q_{t,4}$ are the total flow rates in the producers. As mentioned earlier, the identified model has degrees of freedom, the number of which determines the order of the model, and which can be represented as state variables **x,** linearly related to the inputs **u** and the outputs **y.** Unlike in a physics-based reservoir-simulation model, where the state variables are pressures, saturations, or component concentrations, the states in an identified model do not have a direct physical interpretation. To capture all relevant dynamics in the identified model, the input **u** must be "persistently exciting" during the length of the identification experiment, meaning that all relevant reservoir dynamics need to be stimulated by the inputs (Ljung 1999). Design of such an experiment, in terms of the amplitude, frequencies, and length of the input **u,** can be performed on the basis of a physics-based large-scale reservoir-simulation model and subsequently applied to the real reservoir. This approach was conceptually also adopted in the example presented in this paper, although we used a synthetic "truth" in the form of a second, more detailed, reservoir-simulation model.

Model Predictive Control in Waterflooding

The model predictive controller, as indicated in Fig. 1, acts as a tracking controller for the reference variables obtained from the life-cycle optimization. As usual, the life-cycle optimization aims at maximizing NPV defined as an economic objective function J, which, for our example, becomes

$$J = \sum_{k=1}^{K} \left\{ \frac{\sum_{i=1}^{8} r_{wi} \times (q_{wi,i})_k + \sum_{j=1}^{4} [r_{wp} \times (q_{wp,j})_k + r_o \times (q_{o,j})_k]}{(1+b)^{\frac{t_k}{\tau_t}}} \times \Delta t_k \right\}, \qquad \cdots\cdots\cdots\cdots\cdots\cdots (3)$$

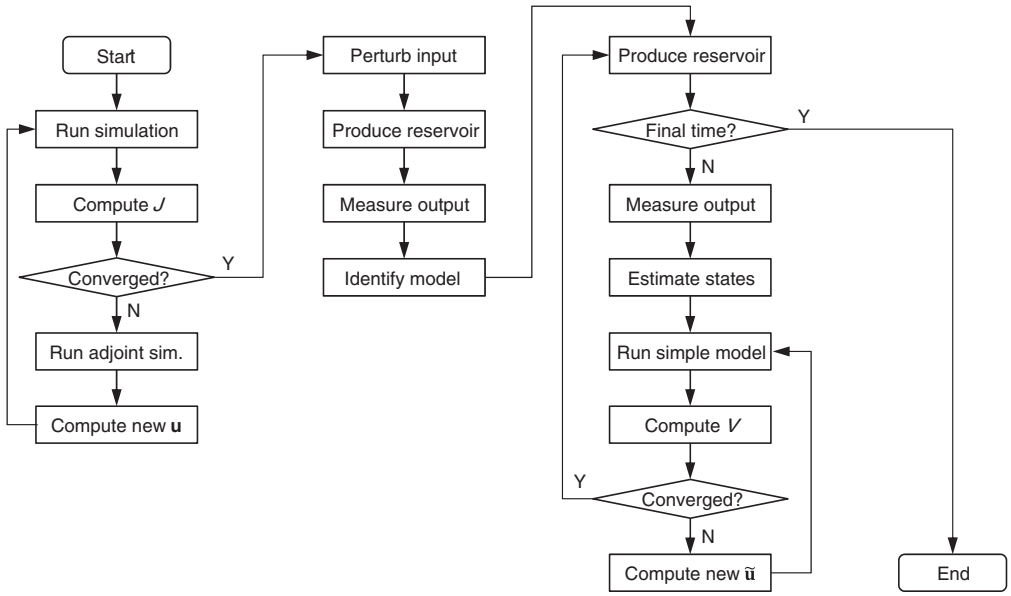

Fig. 2—Flow chart of the two-level strategy. The left column represents life-cycle optimization by use of a large-scale reservoir-simulation model (performed only once in our example). The second column represents identification of a data-driven model (also performed only once in our example). The third column represents computation of tracking control input by use of the identified model.

where $k = 1, 2, \ldots, K$ are the timesteps in the simulator, $q_{wi,i}$ are the water-injection rates of well i, $q_{wp,j}$ are the water-production rates of well j, $q_{o,j}$ are the oil-production rates of well j, r_{wi} are the water-injection costs, r_{wp} are the water-production costs, r_o is the oil revenue, Δt_k is the time interval of timestep k, and b is the discount rate (expressed as a fraction) for a reference time τ_t. During the life-cycle optimization procedure, the input vectors $\mathbf{u}_{1:K}$ are iteratively changed until a maximum value of J is obtained. [The notation $\mathbf{u}_{1:K}$ indicates the set of input vectors over the entire simulation period: $\mathbf{u}_{1:K} = (\mathbf{u}_1, \mathbf{u}_2, \ldots \mathbf{u}_K)$.] Usually, the optimal input vector $\hat{\mathbf{u}}_{1:K}$ (where the hat indicates optimality with respect to the life-cycle reservoir model) is the desired result of the life-cycle optimization procedure. Here, however, we choose the corresponding optimal output $\hat{\mathbf{y}}_{1:K}$ as the result and use this set of optimal total flow rates as the reference variables for the model-predictive controller. The controller now attempts to find corrected inputs $\tilde{\mathbf{u}}$ such that the difference between the data-driven model outputs $\tilde{\mathbf{y}}$ and the life-cycle model-optimal outputs $\hat{\mathbf{y}}$ is minimal. This is achieved by minimizing the following objective function over a relatively short-time moving horizon:

$$V(\tilde{\mathbf{u}}_{k:k+N}) = \sum_{j=k}^{k+N} (\tilde{\mathbf{y}}_j - \hat{\mathbf{y}}_j)^T \mathbf{W}_1 (\tilde{\mathbf{y}}_j - \hat{\mathbf{y}}_j) + (\tilde{\mathbf{u}}_j - \hat{\mathbf{u}}_j)^T \mathbf{W}_2 (\tilde{\mathbf{u}}_j - \hat{\mathbf{u}}_j), \quad \ldots\ldots\ldots\ldots\ldots\ldots (4)$$

where N is the number of timesteps over the moving control horizon and $\mathbf{W}_1$ and $\mathbf{W}_2$ are optional weighting matrices. Note that here, for simplicity, it is assumed that the timesteps k for the life-cycle optimization have the same length as those in the model-predictive controller. In reality, the latter will use much smaller timesteps. The second term at the right side of Eq. 4 ensures that the corrected inputs $\tilde{\mathbf{u}}_{k:k+N}$ do not deviate too much from the optimal inputs $\hat{\mathbf{u}}_{k:k+N}$ as computed in the life-cycle optimization step. The weighting matrices $\mathbf{W}_1$ and $\mathbf{W}_2$ are of relevance for optimization in a stochastic setting, in which case they could be on the basis of the (estimated) uncertainty in the inputs and outputs of the life-cycle and the black-box models. In a deterministic case, as discussed in this paper, they can be used to weight the magnitudes of inputs of a different physical nature, such as pressures and flow rates. The prediction of the output $\tilde{\mathbf{y}}_{k:k+N}$ over the control horizon is performed with the aid of the identified (i.e., data-driven) model. Because the SubID method results in a model with a (small) number of internal state variables **x,** it is necessary to specify initial conditions $\mathbf{x}_k$ at the start of the minimization of V. These can be estimated from the known inputs $\tilde{\mathbf{u}}_{k-1}$ and the measured outputs $\mathbf{y}_{k-1}$ with the aid of a so-called state estimator or observer. Further details of the identification and MPC procedures will be discussed in the example that follows. It should be noted that because in our example the number of inputs is twice the number of outputs, the minimization problem may become ill-posed. Only part of the control input $\tilde{\mathbf{u}}_{k:k+N}$ will then be implemented, after which the process from state estimation to input implementation is repeated. As the real reservoir moves away from the state it was in when the linear data-driven model was created, the prediction accuracy of the model will decrease and reidentification is required. In doing so, the benefit of improved prediction accuracy must be evaluated against the drop in tracking performance during the experiment. However, how to determine the best time to start another remodeling experiment is not explored in this work, but will be the subject of future research. **Fig. 2** depicts a flow chart of the two-level strategy.

Example

The reservoir considered in our example is depicted in **Fig. 3.** Its geological structure is dominated by two intersecting high-permeability channels. The remaining reservoir properties can be found in **Table 1.** The life cycle of the reservoir covers a period of 11.5 years. Of this reservoir a large-scale model was created to serve as the synthetic "truth." To provide realistic predictions of short-term dynamic behavior of the reservoir, a very fine spatial discretization around the wells was adopted and a relatively short time-step size was chosen of 0.25 days. This truth model was used to generate synthetic (noise-free) production measurements, and to assess the "true" production performance over the life of the reservoir. A second reservoir model was created that serves as the model to perform life-cycle optimization and design the identification experiment. No grid refinement around the wells was used, and a timestep size of 30 days was adopted. Besides the coarser discretization in space and time, the second model deviates from the "truth" in its geological structure. In particular, it has channels in a slightly different flow direction, such that different wells are inside the high-permeability streaks (Fig. 3). We used a fully implicit in-house reservoir simulator with adjoint functionality (Kraaijevanger et al. 2007).

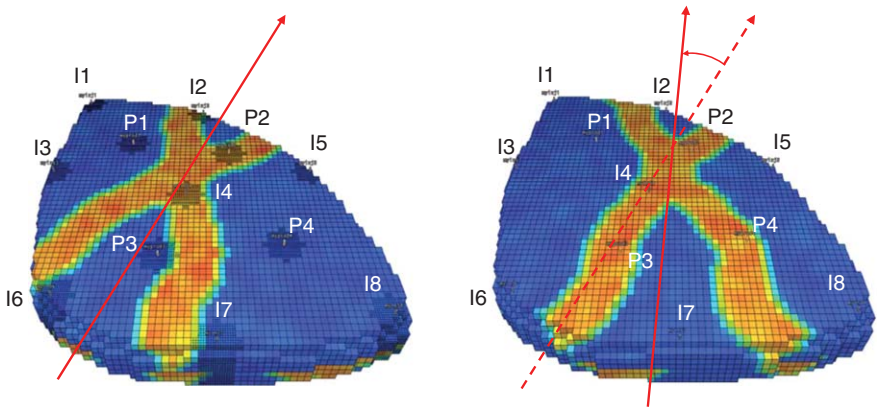

Fig. 3—3D reservoir model (left), used as synthetic "truth," with eight injection wells and four production wells. Its geological structure involves a network of meandering channels of high permeability. The model to the right is used for life-cycle optimization and differs from the model to the left in the direction of the channels, the absence of grid refinement, and the larger timestep size of 30 days.

Economic Life-Cycle Optimization

In the control structure as shown in Fig. 1, the optimal (reference) output $\hat{\mathbf{y}}_{1:K}$ is determined by the life-cycle optimizer by use of objective function 3. We used oil revenues r_o equal to USD 56.6/m^3, water-production costs r_{wp} of USD 6.3/m^3, zero water-injection costs, and an annual discount rate b equal to 0.1. We solved the life-cycle optimization problem with the aid of a gradient-based algorithm for which the gradients were obtained with the adjoint formalism in the simulator (Kraaijevanger et al. 2007). We applied rate constraints to the injectors (a maximum rate of 1590 m^3/d) and pressure constraints to the producers [a minimum bottomhole pressure of 375 bar (i.e., 25 bar below the initial reservoir pressure)]. Solving the life-cycle optimization problem resulted in an expected maximum NPV of USD 596×10^6.

System Identification

System identification was performed on the "true" reservoir. The inputs were the water-injection rates of the eight injectors and the bottomhole pressures of the four producers. The waterflooding process is nonlinear, and as a result the prediction accuracy of a linear model will decrease when the prediction horizon increases. However, in this first experiment, we only once identified a linear model at the start of production for simplicity reasons. The duration of the experiment was chosen by use of the rule of thumb as used in the process industry, such that the length should minimally be five times greater than the largest time constant. Through step-response analysis on the reservoir model (i.e., not on the "truth"), the largest time constant was estimated and the minimal duration of the experiment was estimated at 75 days. (The time constants of a strongly dissipative system such as an oil reservoir can be interpreted as the half-time in output—e.g., the pressure response in a well—following a step change in the input—e.g., the well rate.) For the inputs q_{wi} and p_{wf} to the "real" reservoir, random binary signals (RBSs) were generated. RBSs were used in this experiment because they cover a wide spectrum of frequencies, which makes them suitable to generate a persistently exciting input. From step responses of the reservoir model to each input, it was found that the response to changes in q_{wi} were much slower than responses to changes in p_{wf}. To amplify the low-frequency content of excitation signal of the injection rates, the clock period of the RBS was set to three sample times of 0.25 days. The amplitudes of the RBSs were set to 1590 m^3/d and 1 bar for q_{wi} and p_{wf}, respectively, by use of the reservoir model to determine that the effect on the outputs was significant.

To maintain good economic performance, the RBSs with zero mean were superimposed upon the preferred inputs, which were taken equal to $\hat{\mathbf{u}}$ (i.e., the optimal inputs as obtained from the life-cycle optimization). However, whenever addition of the RBS led to infeasibility with respect to the well constraints, the mean value was moved up or down until feasibility was restored. In the identification experiment, the first 25 days of data were omitted, after which all initialization effects had died out. The excitation signals and the optimal inputs $\hat{\mathbf{u}}$ can be observed in **Fig. 4.** The sampling frequency of the measured outputs $\mathbf{y}$ is determined by the timestep size of the "truth model," which in this example was equal to 0.25 days. The identification experiment was conducted in open loop, because the depletion process is inherently stable. On the basis of these data, an eighth-order SubID model was identified. **Fig. 5** shows the model fit of the model with respect to the measured output data for all four producers. It can be observed that the output of the identified model has a satisfactory accuracy, which illustrates that the eighth-order model is capable of representing all relevant dynamics.

TABLE 1—GEOLOGICAL AND FLUID PROPERTIES FOR EXAMPLE

Property	Value	Units
ϕ	0.20	—
ρ_o (at 1 bar)	800	kg/m^3
ρ_w (at 1 bar)	1000	kg/m^3
c_o	15×10^{-5}	1/bar
c_w	4×10^{-5}	1/bar
μ_o	4×10^{-3}	Pa·s
μ_w	1×10^{-3}	Pa·s
p_{cow}	0	bar
S_{wc}	0.20	—
S_{or}	0.05	—
k_{ro}	0.80	—
k_{rw}	0.92	—
n_o	4.75	—
n_w	3.00	—

MPC

MPC involves minimization of a cost function, as described by Eq. 4. Recall that the outputs are defined as the four total liquid rates in the producers, whereas the inputs are the four bottomhole pressures in the producers and the eight water rates in the injectors. Matrix $\mathbf{W}_1$ (weighting the difference between the optimal long-term outputs $\hat{\mathbf{y}}_{k:k+N}$ and the predicted short-term outputs $\tilde{\mathbf{y}}_{k:k+N}$) was taken as a unit matrix. Weighting matrix $\mathbf{W}_2$ (weighting the difference between the optimal long-term inputs $\hat{\mathbf{u}}_{k:k+N}$ and the predicted short-term inputs $\tilde{\mathbf{u}}_{k:k+N}$) was chosen as a diagonal matrix with zeros and ones in positions corresponding to pressures and flow rates, respectively. As a result, $\mathbf{W}_2$ only penalizes deviations of the optimal injection rates and not of the optimal

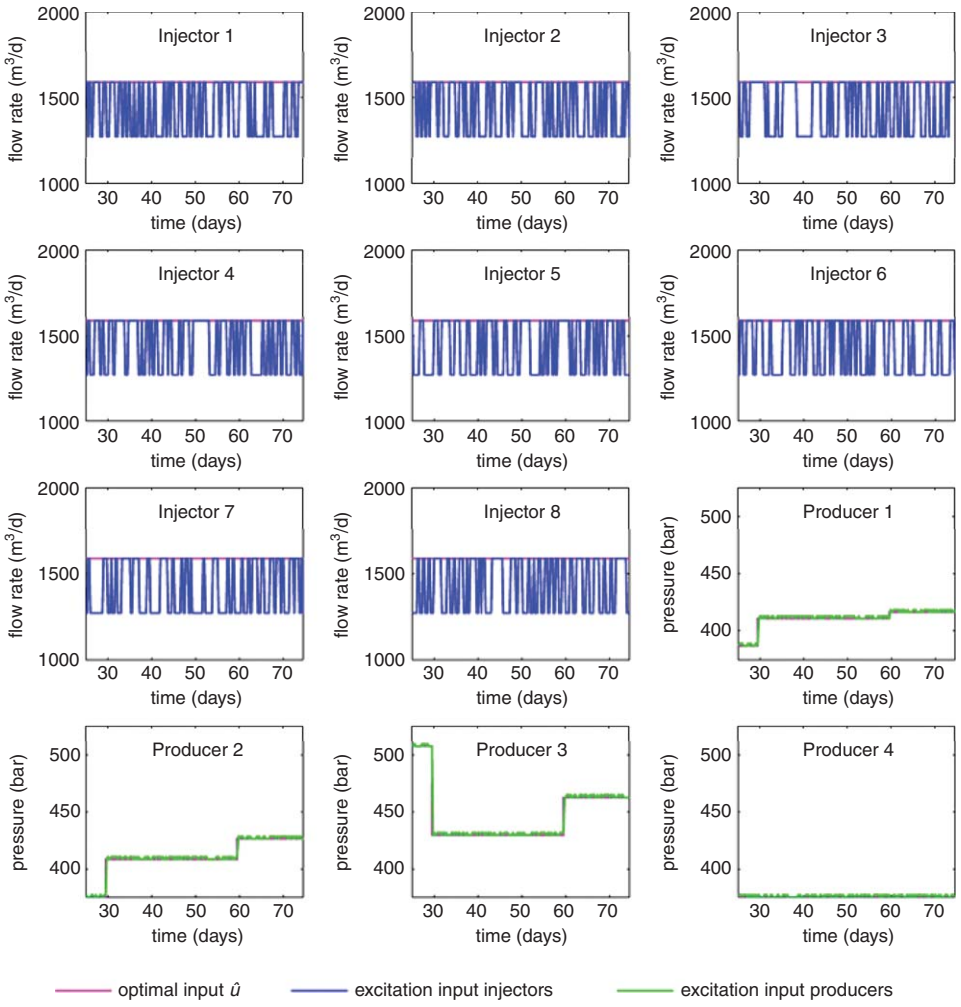

Fig. 4—Excitation signal for the identification experiment along with optimal inputs $\hat{u}$ for each input.

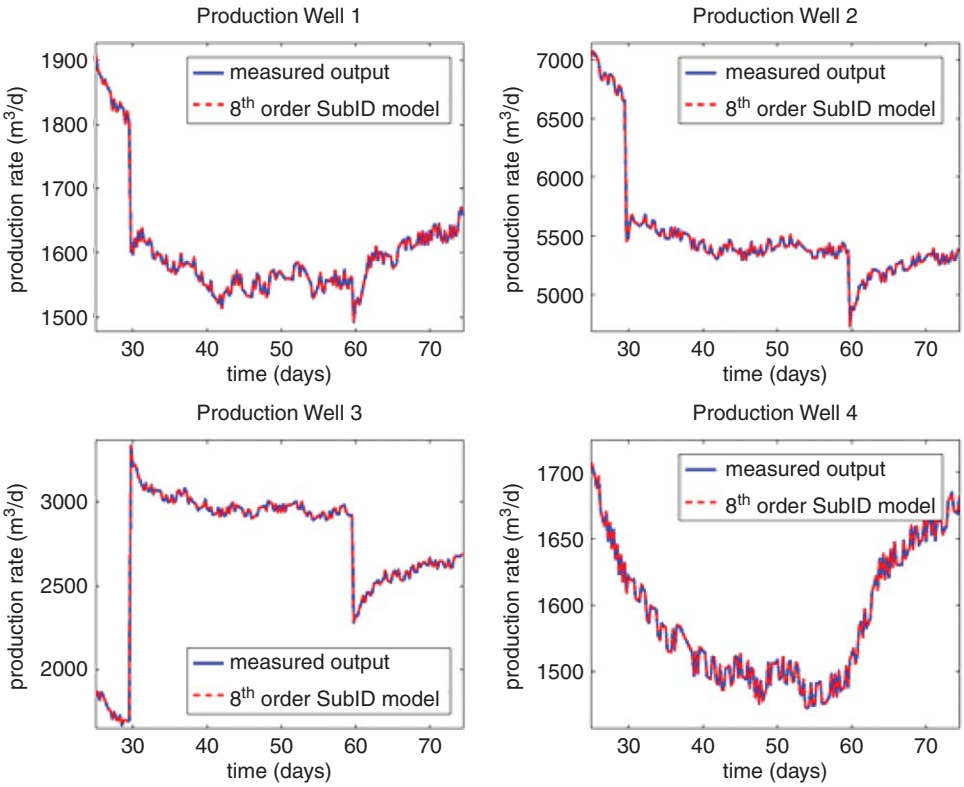

Fig. 5—Model fit of the eighth-order SubID model with respect to the measured output data.

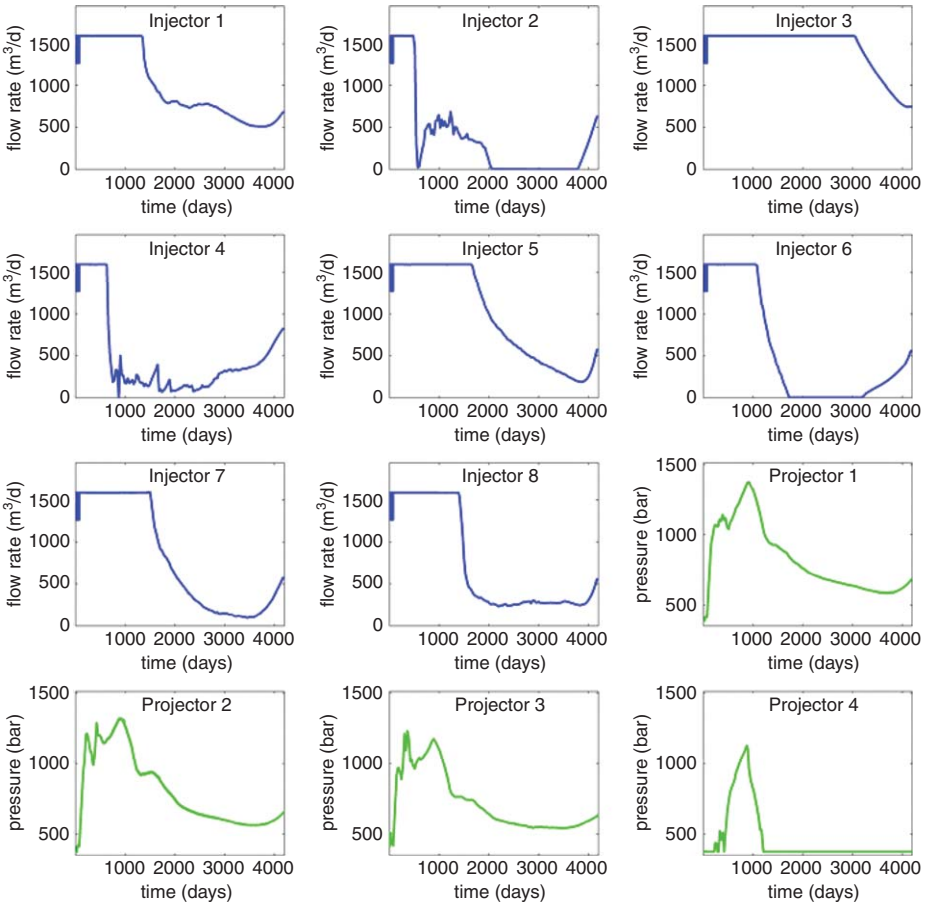

Fig. 6—Controls $\tilde{u}$ as determined by the MPC tracker.

production pressures, such that tracking is mainly realized through changes in the bottomhole pressures in the production wells. The reason behind this choice was to aim for a higher penalty on changes in produced and injected volumes (with the aid of $\mathbf{W}_1$ and the nonzero elements of $\mathbf{W}_2$, respectively), than on changes in the corresponding pressures. In this experiment, the prediction horizon N was chosen equal to 28 (i.e., 1 week). For each timestep, the minimization problem is solved for the (moving) prediction horizon, which involves two sequential steps: state estimation and quadratic programming (QP).

State Estimation. In this simulation study, no artificial noise was added to the measurements. As a result, the state-estimation problem can be attacked quite straightforwardly using a Luenberger observer (Friedland 1986); Appendix B provides further details. Note, however, that alternative choices for state estimation may be considered (e.g., Kalman filtering).

QP. To solve the minimization of objective function V subject to the inequality constraints on the inputs, a QP problem needs to be solved. In this experiment, a gradient-based QP solver was used, implemented in the in-house reservoir simulator.

We note that the particular algorithmic choices for Steps 1 and 2 have little impact on the MPC tracking procedure. The controls $\tilde{\mathbf{u}}_{k:k+N}$ as determined by the MPC tracker were recalculated and applied to the "real" reservoir at every 0.25-day timestep **(Fig. 6).**

Results

We compare the results from inputs $\tilde{\mathbf{u}}$ obtained with the additional MPC layer to results from direct, open-loop application of optimal inputs $\hat{\mathbf{u}}$. Performance is evaluated in terms of both tracking performance and NPV. Tracking performance can be observed in **Fig. 7.** In **Table 2,** the NPVs of the open-loop application of $\hat{\mathbf{u}}$ and $\tilde{\mathbf{u}}$ are shown in comparison with the expected maximum NPV determined by the life-cycle optimizer. Fig. 7 depicts the reference and output trajectories for both the open-loop and the MPC-tracked case for each of the four production wells over the life of the field. In each of the four plots, four different stages can be identified. In the first 75 days of production, the identification experiment is conducted where the optimal inputs $\hat{\mathbf{u}}$ serve as mean values. During this period, the error is large because of the model error between the reservoir model and the "truth," whereas the MPC tracker is not active yet. From 75 to approximately 500 days, tracking performance is good because of activation of the MPC tracker. After 500 days, tracking performance decreases, but still outperforms open-loop control. This drop is the result of water breakthrough in the production wells, which has a strong nonlinear effect on the dynamics. After approximately 3,000 days, tracking improves again, because mainly water is produced, resulting in a more linear response to the inputs.

Discussion

Theoretical Aspects. In this example, we used noise-free measurements, which is of course an unrealistic assumption. The SubID and MPC steps can also be performed in a stochastic setting, taking into account measurement noise and model errors, and it is to be expected that increased noise levels will result in a reduced performance of our proposed method. On the other hand, in this example we did only once determine the SubID model used as a basis for the MPC tracker, and we may expect an improved tracking performance when frequent re-estimation of the SubID model is conducted over the length of the field's life cycle. Moreover, we did not apply any CAHM to update the reservoir model used for the life-cycle optimization. Nor did we use robust optimization (i.e., optimization based on multiple models

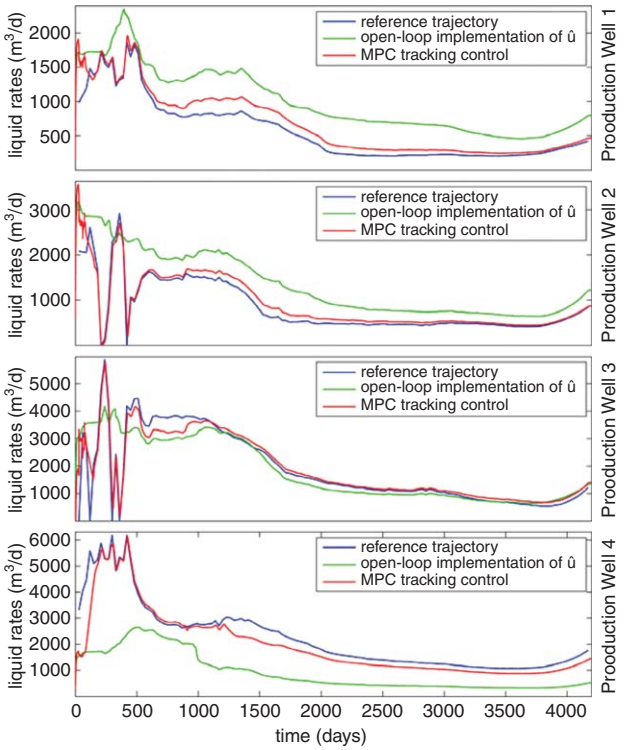

Fig. 7—Reference and output trajectories for the open-loop application and the tracked case for each of the four production wells over the life of the field.

to reduce the sensitivity to geological uncertainties). Therefore, the only way to counteract the negative effects of model inaccuracies on the life-cycle performance of the "true" reservoir was through the actions of the model predictive tracking controller. On the basis of experiences in the process industry, we know that such a tracking control approach is effective when the disturbances are local in time or space, and can, mathematically, be considered as perturbations around a nominal control trajectory, but with possibly significant cumulative effects. In that case, the long-term model-based optimal result that is used as reference can still be considered a valid approximation for the real, disturbed, situation. In our example, the disturbances resulted from two sources: near-wellbore effects, which were not captured (neither in space nor in time) in the reservoir model used for the life-cycle optimization, and a small shift in channel orientation. These model errors result in disturbances that apparently, in this example, were small enough to be rejected by the tracking algorithm. Thus, it was possible to realize a life-cycle production response, in the presence of disturbances, that closely resembled the model-optimal results. The reason to use a physics-based model for life-cycle optimization is that a data-driven model can never predict water breakthrough or, more generally, saturations. Data-driven models can, however, very well predict pressures over a limited horizon during which the saturations do not change significantly. The effect of small "disturbances" (in terms of operational events or differences between model and reality) that cause small pressure differences can therefore be "rejected" (i.e., compensated for by control actions on the basis of a data-driven model). Rejection of larger disturbances, which significantly affect the saturations in the reservoir and/or the water-breakthrough times in the wells, would require more-time-consuming updates of the physical reservoir model (e.g., through CAHM and/or geological-model revision). In practice, it will be difficult to estimate the magnitude of the disturbances, and therefore to know whether the use of a tracking controller on its own will be sufficient to counteract these. Therefore, it seems a logical step to combine tracking control with robust optimization and/or closed-loop reservoir management, resulting in a two-level approach with two feedback loops, as indicated in **Fig. 8.** In such a setting, the lower-level tracking controller would quickly take care of local disturbances, either in space or in time, not captured in the upper-level reservoir model(s), whereas the more-time-consuming CAHM and the use of multiple models would account for larger-scale model errors.

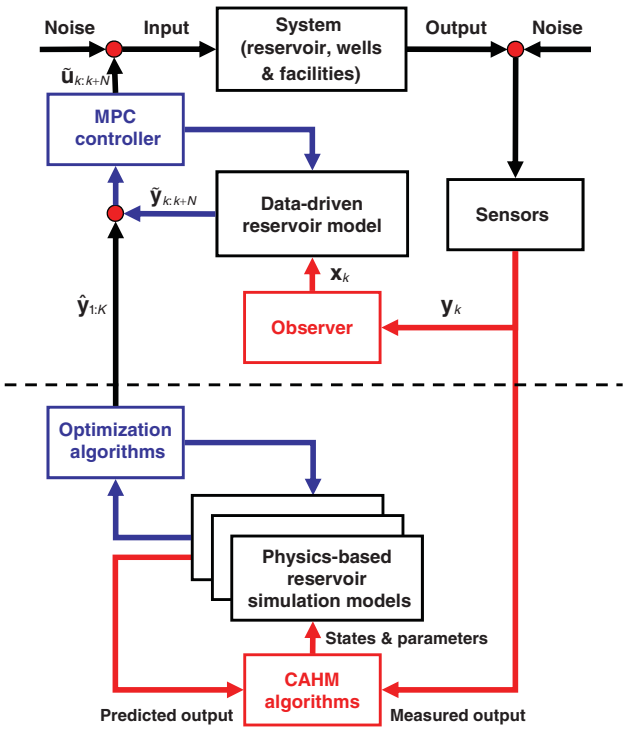

Fig. 8—Two-level strategy to combine closed-loop reservoir management based on multiple models (bottom part of the figure) with tracking control of production (top part of the figure).

TABLE 2—ECONOMIC PERFORMANCE

	NPV	% Change
Maximum predicted	USD 596×10^6	—
Open-loop application of $\hat{\mathbf{u}}$	USD 558×10^6	−6.4%
MPC tracking using $\tilde{\mathbf{u}}$	USD 594×10^6	−0.5%

Practical Aspects. The creation of a data-driven model requires manipulation of the inputs of the system. In our setting, this implies changing the rates or pressures (either at the wellhead or downhole) in the wells. To maximize the information content in the resulting outputs (i.e., measured pressures and rates), a "persistently exciting" input signal is required. The required excitation frequency should be high enough to capture typical near-wellbore transients. In our example, this translated to a frequency of 0.25 days (i.e., once every 6 hours). Such a frequency is too high for manual operation but should pose no problems for automatic (computer-operated) surface control valves, as are standard in the process industry. The required amplitude is dependent on the signal-to-noise ratio in the measured outputs. This leads to a tradeoff between maximizing the excitation amplitude and the measurement time interval, which both result in a better signal/noise ratio. Note that it is not necessary to implement the input fluctuations as an on/off sequence but that they may consist of a relatively low-amplitude fluctuation on top of a steady-state signal. This latter feature may make a practical implementation in a producing asset more acceptable. Moreover, in cases where manipulation of producing-well parameters is operationally unacceptable, the input fluctuations could be restricted to the water injectors only, at the price of reduced information content in the measurements.

Conclusions

The introduction of a two-level optimization and control strategy as described in this paper, combining life-cycle optimization with tracking control, was aimed at rapid attenuation of disturbances caused by small geological and near-wellbore model errors. For the example considered, we conclude that

- It is possible to obtain a linear data-driven reservoir model through system identification, which gives accurate predictions for a time horizon that is relatively short, but long enough to realize tracking control.
- Tracking control is capable of quickly rejecting the disturbances resulting from small model errors in the form of neglected near-wellbore effects and a slightly erroneous channel orientation.
- The disturbance rejection results in a life-cycle production response that closely resembles the model-optimal results.

Further research is required to assess the range of validity of this approach, in particular in combination with alternative methods to counteract the negative effects of model errors on life-cycle optimization, such as robust optimization or closed-loop reservoir management.

Nomenclature

b = discount rate, t^{-1}, 1/year
c = compressibility, $m^{-1}\ L\ t^2$, 1/bar
j = timestep counter for moving horizon
J = objective function, USD
k = discrete time, or permeability, L^2, md
K = total number of timesteps
n = Corey exponent
N = number of timesteps in moving horizon
p = pressure, $m\ L^{-1}\ t^{-2}$, Pa
q = flow rate, m^3/d
r = unit revenue/cost, USD/m^3
S = saturation
t = time, t, days
$\mathbf{u}$ = input vector
$\tilde{\mathbf{u}}$ = data-driven model-generated input vector
$\hat{\mathbf{u}}$ = life-cycle model-generated input vector
V = objective function
$\mathbf{W}$ = weighting matrix
$\mathbf{x}$ = state vector
$\mathbf{y}$ = output vector
$\tilde{\mathbf{y}}$ = data-driven model-generated output vector
$\hat{\mathbf{y}}$ = life-cycle model-generated output vector
μ = viscosity, $m\ L^{-1}\ t^{-1}$, Pa·s
ρ = density, $L^{-3}\ m$, kg/m^3
τ = reference time, t, days
ϕ = porosity

Subscripts

cow = capillary (oil/water)
ro = relative, oil
rw = relative, water
t = total
o = oil
wf = flowing wellbore
wi = injected water
wp = produced water

Superscripts

T = transposed

Acknowledgments

We thank Amin Rezapour (now a PhD student at the University of Southern California, Los Angeles, California) for his contributions to this paper, which formed part of his MSc thesis project. We acknowledge Shell for the use of their in-house reservoir simulator MoReS. This research was carried out within the context of the Integrated Systems Approach to Petroleum Production knowledge center, a joint project of Delft University of Technology, Shell International Exploration and Production, and the Netherlands Organization for Applied Scientific Research TNO.

References

Alhuthali, A.H., Oyerinde, D. and Datta-Gupta, A. 2007. Optimal Waterflood Management Using Rate Control. *SPE Res Eval & Eng* **10** (5) 539–551. http://dx.doi.org/10.2118/102478-PA.

Almeida, L.F., Tupac, Y.J., Lazo Lazo, J.G., et al. 2007. Evolutionary Optimization of Smart-Wells Control Under Technical Uncertainties. Paper SPE 107872 presented at the Latin American and Caribbean Petroleum Engineering Conference, Buenos Aires, Argentina, 15–18 April. http://dx.doi.org/10.2118/107872-MS.

Asheim, H. 1988. Maximization of Water Sweep Efficiency by Controlling Production and Injection Rates. Paper SPE 18365 presented at the SPE European Petroleum Conference, London, United Kingdom, 16–18 October. http://dx.doi.org/10.2118/18365-MS.

Brouwer, D.R. and Jansen, J.D. 2004. Dynamic Optimization of Water Flooding with Smart Wells Using Optimal Control Theory. *SPE J.* **9** (4): 391–402. http://dx.doi.org/10.2118/78278-PA.

Chen, C., Li, G. and Reynolds, A.C. 2012. Robust Constrained Optimization of Short- and Long-Term Net Present Value for Closed-Loop Reservoir Management. *SPE J.* **17** (3): 849–864. http://dx.doi.org/10.2118/141314-PA.

Chen, Y., Oliver, D.S. and Zhang, D. 2009. Efficient Ensemble-Based Closed-Loop Production Optimization. *SPE J.* **14** (4): 634–645. http://dx.doi.org/10.2118/112873-PA.

Chierici, G.L., Gottardi, G.A. and Guidorzi, R.P. 1981. Identified Models for Gas Storage Dynamics. *SPE J.* **21** (2) 151–159. http://dx.doi.org/10.2118/8862-PA.

Echeverría Ciaurri, D., Mukerji, T. and Durlofsky, L.J. 2011. Derivative-Free Optimization for Oil Field Operations. In: *Computational Optimization and Applications in Engineering and Industry*, eds. Berlin. X. S. Yang and S. Koziel, 19–55. Studies in Computational Intelligence Series, Springer-Verlag.

Foss, B. and Jensen, J.P. 2010. Performance Analysis for Closed-Loop Reservoir Management. *SPE J.* **16** (1) 183–190. http://dx.doi.org/10.2118/138891-PA.

Friedland, B. 1986. *Control System Design: An Introduction to State Space Methods*. New York City, New York: McGraw Hill.

Heijn, T., Markovinovic, R. and Jansen, J.D. 2004. Generation of Low-Order Reservoir Models Using System-Theoretical Concepts. *SPE J.* **9** (2): 202–218. http://dx.doi.org/10.2118/88361-PA.

Jansen, J.D., Douma, S.G., Brouwer, D.R., et al. 2009. Closed-Loop Reservoir Management. Paper SPE 119098 presented at the SPE Reservoir Simulation Symposium, The Woodlands, Texas, 2–4 February. http://dx.doi.org/10.2118/119098-MS.

Jansen, J.D. 2011. Adjoint-Based Optimization of Multiphase Flow Through Porous Media – A Review. *Comput. Fluids* **46** (1): 40–51. http://dx.doi.org/10.1016/j.compfluid.2010.09.039.

Kraaijevanger, J.F.B.M., Egberts, P.J.P., Valstar, J.R., et al. 2007. Optimal Water Flood Design Using the Adjoint Method. Paper SPE 105764 presented at the SPE Reservoir Simulation Symposium, Houston, 26–28 February. http://dx.doi.org/10.2118/105764-MS.

Liu, F., Mendel, J.M. and Nejad, A.M. 2009. Forecasting Injector/Producer Relationships from Production and Injection Rates Using an Extended Kalman Filter. *SPE J.* **14** (4): 653–664. http://dx.doi.org/10.2118/110520-PA.

Ljung, L. 1999. *System Identification - Theory for the User*, second edition. Upper Saddle River, New Jersey: Prentice-Hall.

Markovinovic, R., Geurtsen, E.L. and Jansen, J.D. 2002. Subspace Identification of Low-Order Reservoir Models. Proc. XIV International Conference on Computational Methods in Water Resources, Delft, the Netherlands, 23–28 June, 281–288.

Naevdal, G., Brouwer, D.R. and Jansen, J.D. 2006. Water Flooding Using Closed-Loop Control. *Computat. Geosci.* **10** (1): 37–60. http://dx.doi.org/10.1007/s10596-005-9010-6.

Rowan, G. and Clegg, M.W. 1963. The Cybernetic Approach to Reservoir Engineering. Paper SPE 727 presented at the 38th Annual Fall Meeting of the SPE of AIME, New Orleans, Louisiana, 6–9 October. http://dx.doi.org/10.2118/727-MS.

Saputelli, L., Nikolaou, M. and Economides, M.J. 2006. Real-Time Reservoir Management: A Multi-Scale Adaptive Optimization and Control Approach. *Computat. Geosci.* **10** (1): 61–96. http://dx.doi.org/10.1007/s10596-005-9011-5.

Sarma, P., Aziz, K. and Durlofsky, L.J. 2005. Implementation of Adjoint Solution for Optimal Control of Smart Wells. Paper SPE 92864 presented at the SPE Reservoir Simulation Symposium, Houston, Texas, 31 January–2 February. http://dx.doi.org/10.2118/92864-MS.

Sarma, P., Durlofsky, L.J. and Aziz, K. 2008. Computational Techniques for Closed-Loop Reservoir Modeling with Application to a Realistic Reservoir. *Pet. Sci. Tech.* **26** (10–11):1120-1140. http://dx.doi.org/10.1080/10916460701829580.

Sayarpour, M., Zuluaga, E., Kabir, C.S., et al. 2009. The Use of Capacitance–Resistance Models for Rapid Estimation of Waterflood Performance and Optimization. *J. Pet. Sci. Eng.* **69** (3–4): 227–238. http://dx.doi.org/10.1016/j.petrol.2009.09.006.

Su, H-J. and Oliver, D.S. 2010. Smart-Well Production Optimization Using an Ensemble-Based Method. *SPE Res Eval & Eng* **13** (6): 884–892. http://dx.doi.org/10.2118/126072-PA.

Sudaryanto, B., and Yortsos, Y.C. 2000. Optimization of Fluid Front Dynamics in Porous Media Using Rate Control: I. Equal Fluids. *Phys. Fluids* **12** (7): 1656–1670. http://dx.doi.org/10.2172/13828.

Van Essen, G.M., Zandvliet, M.J., Van den Hof, P.M.J., et al. 2009. Robust Water Flooding Optimization of Multiple Geological Scenarios. *SPE J.* **14** (1): 202–210. http://dx.doi.org/10.2118/102913-PA.

Van Essen, G.M., Van den Hof, P.M.J. and Jansen, J.D. 2011. Hierarchical Long-Term and Short-Term Production Optimization. *SPE J.* **16** (1): 191–199. http://dx.doi.org/10.2118/124332-PA.

Van Overschee, P. and De Moor, B. 1996. *Subspace Identification for Linear Systems: Theory, Implementation, Applications*. Norwell, Massachusetts: Kluwer Academic Publishers.

Viberg, M. 1995. Subspace-Based Methods for the Identification of Linear Time-Invariant Systems. *Automatica* **31** (12): 1835–1851. http://dx.doi.org/10.1016/0005-1098(95)00107-5.

Wang, C., Li, G. and Reynolds, A.C., 2009: Production Optimization in Closed-Loop Reservoir Management. *SPE J.* **14** (3): 506–523. http://dx.doi.org/10.2118/109805-PA.

Appendix A—Subspace Identification

For a detailed overview of subspace identification methods we refer the reader to Viberg (1995), Van Overschee and De Moor (1996), and Ljung (1999). Here, we provide a brief description. Data-driven modeling through subspace methods starts from a system description in state space form, according to

$$\mathbf{x}_{k+1} = \mathbf{A}x_k + \mathbf{B}u_k + \mathbf{w}_k \ldots \quad \ldots\ldots\ldots\ldots\ldots\ldots\ldots \quad (A\text{-}1)$$

$$\mathbf{y}_k = \mathbf{C}\mathbf{x}_k + \mathbf{D}\mathbf{u}_k + \mathbf{v}_k, \ldots \quad \ldots\ldots\ldots\ldots\ldots\ldots\ldots \quad (A\text{-}2)$$

where $k \in \mathbb{N}$ is discrete time, $\mathbf{x} \in \mathbb{R}^{n\times 1}$ is the state vector, $\mathbf{u} \in \mathbb{R}^{m\times 1}$ is the input vector, $\mathbf{y} \in \mathbb{R}^{p\times 1}$ is the output vector, $\mathbf{A} \in \mathbb{R}^{n\times n}$ is the system matrix, $\mathbf{B} \in \mathbb{R}^{n\times m}$ is the input matrix, $\mathbf{C} \in \mathbb{R}^{p\times n}$ is the output matrix, $\mathbf{D} \in \mathbb{R}^{p\times m}$ is the direct throughput matrix, and $\mathbf{w} \in \mathbb{R}^{n\times 1}$ and $\mathbf{v} \in \mathbb{R}^{p\times 1}$ are zero-mean stationary stochastic processes representing system and measurement noise, respectively. The objective of the identification procedure is to determine, on the basis of input and output data $(\mathbf{u}_k, \mathbf{y}_k)_{k=1,\ldots,K}$, a so-called state space realization—i.e., a set of matrices $(\mathbf{A}, \mathbf{B}, \mathbf{C}, \mathbf{D})$, together with the system order (i.e., the dimension n of the state variable $\mathbf{x}$). In subspace identification, the most common approach to achieve this is to

(1) Estimate the so-called extended observability matrix,

$$\mathbf{O}_r = \begin{pmatrix} \mathbf{C} \\ \mathbf{CA} \\ \vdots \\ \mathbf{CA}^{r-1} \end{pmatrix}, \quad \ldots\ldots\ldots\ldots\ldots\ldots\ldots \quad (A\text{-}3)$$

where r is a finite time-horizon to be chosen by the user. On the basis of $\mathbf{O}_r$, the pair $(\mathbf{A}, \mathbf{C})$ can be estimated.

(2) Estimate $(\mathbf{B}, \mathbf{D})$ through a simple least-squares (linear-regression) approach.

Step 1. When writing the output Eq. A-2 for $k, k+1, \ldots, k+r-1$, and denoting the extended vectors,

$$\mathbf{u}_{k|r} \triangleq \begin{pmatrix} \mathbf{u}_k \\ \vdots \\ \mathbf{u}_{k+r-1} \end{pmatrix}, \quad \ldots\ldots\ldots\ldots\ldots\ldots\ldots \quad (A\text{-}4)$$

$$\mathbf{v}_{k|r} \triangleq \begin{pmatrix} \mathbf{v}_k \\ \vdots \\ \mathbf{v}_{k+r-1} \end{pmatrix}, \quad \ldots\ldots\ldots\ldots\ldots\ldots\ldots \quad (A\text{-}5)$$

$$\mathbf{y}_{k|r} \triangleq \begin{pmatrix} \mathbf{y}_k \\ \vdots \\ \mathbf{y}_{k+r-1} \end{pmatrix} \quad \ldots\ldots\ldots\ldots\ldots\ldots\ldots \quad (A\text{-}6)$$

it follows that

$$\mathbf{y}_{k|r} = \mathbf{O}_r x_k + \mathbf{S}_r u_{k|r} + \mathbf{v}_{k|r}, \quad \ldots\ldots\ldots\ldots\ldots\ldots \quad (A\text{-}7)$$

where the (lower-triangular block-Toeplitz) matrix $\mathbf{S}_r$ is given by

$$\mathbf{S}_r = \begin{pmatrix} \mathbf{D} & \mathbf{0} & \cdots & \mathbf{0} \\ \mathbf{CB} & \mathbf{D} & \cdots & \mathbf{0} \\ \vdots & \vdots & \ddots & \vdots \\ \mathbf{CA}^{r-2}\mathbf{B} & \mathbf{CA}^{r-3}\mathbf{B} & \cdots & \mathbf{D} \end{pmatrix}. \quad \ldots\ldots\ldots\ldots \quad (A\text{-}8)$$

With

$$\mathbf{U} \triangleq (\,\mathbf{u}_{1|r} \quad \cdots \quad \mathbf{u}_{K|r}\,), \quad \ldots\ldots\ldots\ldots\ldots\ldots \quad (A\text{-}9)$$

$$\mathbf{V} \triangleq (\,\mathbf{v}_{1|r} \quad \cdots \quad \mathbf{v}_{K|r}\,), \quad \ldots\ldots\ldots\ldots\ldots\ldots \quad (A\text{-}10)$$

$$\mathbf{X} \triangleq (\,\mathbf{x}_1 \quad \cdots \quad \mathbf{x}_K\,), \quad \ldots\ldots\ldots\ldots\ldots\ldots \quad (A\text{-}11)$$

$$\mathbf{Y} \triangleq (\,\mathbf{y}_{1|r} \quad \cdots \quad \mathbf{y}_{K|r}\,) \quad \ldots\ldots\ldots\ldots\ldots\ldots \quad (A\text{-}12)$$

this becomes

$$\mathbf{Y} = \mathbf{O_r}\mathbf{X} + \mathbf{S_r}\mathbf{U} + \mathbf{V}. \quad \ldots\ldots\ldots\ldots\ldots\ldots \quad (A\text{-}13)$$

Estimation of $\mathbf{O_r}$ can now be performed through projections/correlations—i.e., by post-multiplying matrix Eq. A-8 with a matrix $\mathbf{P}$ such that the terms with $\mathbf{U}$ and $\mathbf{V}$ on the right side disappear (in expected value for $K \to \infty$). Then,

$$\mathbf{YP} \approx \mathbf{O_r}\mathbf{XP}, \quad \ldots\ldots\ldots\ldots\ldots\ldots\ldots \quad (A\text{-}14)$$

and the column space of $\mathbf{YP}$ is equal to the column space of $\mathbf{O_r}$, whereas the dimension of this column space is determined by the dimension of $\mathbf{x}$. By decomposing $\mathbf{YP}$ in a singular-value decomposition (SVD),

$$\mathbf{YP} = (\,\mathbf{\Phi}_1 \quad \mathbf{\Phi}_2\,)\begin{pmatrix} \mathbf{\Sigma}_1 & \mathbf{0} \\ \mathbf{0} & \mathbf{\Sigma}_2 \end{pmatrix}\begin{pmatrix} \mathbf{\Psi}_1^T \\ \mathbf{\Psi}_2^T \end{pmatrix}, \quad \ldots\ldots\ldots\ldots \quad (A\text{-}15)$$

and choosing the decomposition in such a way that the dominant singular values are in $\mathbf{\Sigma}_1$ and the smaller singular values in Σ_2, the column space of $\mathbf{O}_r$ is estimated by $\mathbf{\Phi}_1$ whereas the corresponding state dimension is given by the number of singular values in $\mathbf{\Sigma}_1$. From an estimate of $\mathbf{O}_r$, a corresponding estimate of $(\mathbf{A}, \mathbf{C})$ can easily be determined. Note that the SVD actually serves as an order-estimation algorithm.

Step 2. With estimates of matrices $\mathbf{A}$ and $\mathbf{C}$ available (denoted by $\hat{\mathbf{A}}$ and $\hat{\mathbf{C}}$), matrices $\mathbf{B}$ and $\mathbf{D}$ can be found by solving for the linear-regression problem,

$$\min_{\mathbf{B},\mathbf{D}} \frac{1}{K}\sum_{k=1}^{K}\left\|\mathbf{y}_k - \hat{\mathbf{C}}(q\mathbf{I}-\hat{A})^{-1}\mathbf{B}\mathbf{u}_k - \mathbf{D}\mathbf{u}_k\right\|_2^2, \quad \ldots\ldots \text{(A-16)}$$

in which q denotes the shift operator, $q\mathbf{u}_k = \mathbf{u}_{k+1}$.

Subspace methods of system identification have the advantages that they rely on robust numerical tools such as SVD, are simply applicable to multiple-input/multiple-output systems, and incorporate an effective order test.

Appendix B—State Estimation With a Luenberger Observer

An observer is a dynamical system that reconstructs the states of the process under study modeled after measurements of the process inputs and outputs. For the linear time-invariant process determined by the continuous-time state space model,

$$\mathbf{x}_{k+1} = \mathbf{A}\mathbf{x}_k + \mathbf{B}\mathbf{u}_k \quad \ldots\ldots\ldots\ldots\ldots\ldots\ldots\ldots\ldots\ldots \text{(B-1)}$$

$$\mathbf{y}_k = \mathbf{C}\mathbf{x}_k + \mathbf{D}\mathbf{u}_k \quad \ldots\ldots\ldots\ldots\ldots\ldots\ldots\ldots\ldots\ldots \text{(B-2)}$$

the Luenberger observer has the format

$$\hat{\mathbf{x}}_{k+1} = \mathbf{A}\hat{\mathbf{x}}_k + \mathbf{B}\mathbf{u}_k + \mathbf{L}(\mathbf{y}_k - \hat{\mathbf{y}}_k) \quad \ldots\ldots\ldots\ldots\ldots\ldots\ldots \text{(B-3)}$$

$$\hat{\mathbf{y}}_k = \mathbf{C}\hat{\mathbf{x}}_k + \mathbf{D}\mathbf{u}_k \quad \ldots\ldots\ldots\ldots\ldots\ldots\ldots\ldots\ldots\ldots \text{(B-4)}$$

where $\hat{\mathbf{x}}$ is the estimated state and $\hat{\mathbf{y}}$ is the model output, and the observer is specified by choosing an observer gain $\mathbf{L} \in \mathbb{R}^{n\times p}$. Note that the observer is actually a copy of the original process with a correction term that serves to drive the estimated $\hat{\mathbf{x}}$ toward $\mathbf{x}$ in case that the measured output $\mathbf{y}$ deviates from the model output $\hat{\mathbf{y}}$.

For the estimation error $\tilde{\mathbf{x}} = \mathbf{x} - \hat{\mathbf{x}}$, it can be shown that it satisfies the dynamic equation

$$\dot{\tilde{\mathbf{x}}}_{k+1} = (\mathbf{A} - \mathbf{L}\mathbf{C})\tilde{\mathbf{x}}_k. \quad \ldots\ldots\ldots\ldots\ldots\ldots\ldots\ldots\ldots\ldots \text{(B-5)}$$

The observer gain $\mathbf{L}$ is chosen to have convergence of the estimation error to zero with sufficient "speed" as the overshoot of the error response stays limited.

Gijs van Essen works as a research reservoir engineer at Shell Global Solutions International. He is conducting a PhD project at Delft University of Technology, Delft, the Netherlands, on production optimization and reservoir management. Van Essen holds an MSc degree in systems and control engineering from Delft University of Technology.

Paul Van den Hof is Professor of Control Systems in the Department of Electrical Engineering at Eindhoven University of Technology, Eindhoven, the Netherlands, and scientific director of the Dutch Institute of Systems and Control. His current research interests are in system identification and model-based control and optimization, with applications in several technology domains, including petroleum reservoir-engineering systems.

Jan-Dirk Jansen is Professor of Reservoir Systems and Control and Head of the Department of Geoscience and Engineering at Delft University of Technology, the Netherlands. His current research interests are the use of systems and control theory for production optimization and reservoir management. Jansen previously worked for Shell International in research and operations.